

Non-zero Yarkovsky acceleration for near-Earth asteroid (99942) Apophis

Jorge A. Pérez-Hernández^{1✉} & Luis Benet¹  ^{1✉}

The leading source of uncertainty to predict the orbital motion of asteroid (99942) Apophis is a non-gravitational acceleration arising from the anisotropic thermal re-emission of absorbed radiation, known as the Yarkovsky effect. Previous attempts to obtain this parameter from astrometry for this object have only yielded marginally small values, without ruling out a pure gravitational interaction. Here we present an independent estimation of the Yarkovsky effect based on optical and radar astrometry which includes observations obtained during 2021. Our numerical approach exploits automatic differentiation techniques. We find a non-zero Yarkovsky parameter, $A_2 = (-2.899 \pm 0.025) \times 10^{-14}$ au d⁻², with induced semi-major axis drift of (-199.0 ± 1.5) m yr⁻¹ for Apophis. Our results provide definite collision probability predictions for the close approaches in 2029, 2036, and 2068.

¹Instituto de Ciencias Físicas, Universidad Nacional Autónoma de México, Av. Universidad s/n, Col. Chamilpa, CP 62210 Cuernavaca, Mor., Mexico.
✉email: jperez@icf.unam.mx; benet@icf.unam.mx

Apophis (99942), a Near Earth Asteroid (NEA) discovered in 2004, will have a close approach to the Earth on April 13, 2029, with a proximity close to 1/10 of the Earth-Moon distance^{1,2}. Computing the orbital dynamics of a NEA is a difficult problem, especially for assessing possible hazardous events where high precision is crucial: the NEA orbit is sensitive to several interactions, including post-Newtonian gravitational corrections, tidal effects and non-gravitational forces^{3,4}. The leading source of orbital uncertainty for Apophis is the Yarkovsky effect^{2,5–7}, a dissipating non-gravitational interaction which induces a semi-major axis acceleration due to re-emission of the incident solar radiation^{8–11}. Several attempts to obtain this acceleration for Apophis have reported marginal detections, essentially indistinguishable from a pure gravitational model^{7,12–14}.

Here we report independent results for a non-zero value of the unknown transverse Yarkovsky acceleration of Apophis, as determined from optical and radar astrometry data that include 2021 observations. Our results provide definite predictions for the close approach in 2029 of Apophis, as well as in 2036 and 2068. The results use an independent implementation for the planetary ephemeris and for the orbital dynamics of Apophis, as well as a different numerical integration technique. The value we obtain is essentially the same as the current one reported by the Jet Propulsion Laboratory (JPL)¹ with minor differences in the uncertainties, and is also consistent with preliminary estimates which use high-quality optical observations¹⁵. While the underlying ephemeris and NEA models differ, the agreement of the values is a reproducible validation for the calculations, which is particularly important and desirable specially for potentially hazardous objects.

Results and discussion

Very precise ephemerides are required to compute possible hazardous events of NEAs. This imposes having a realistic model for the Solar System dynamics and for the asteroid. We have implemented a planetary model to compute high-precision ephemeris of the major Solar System objects¹⁶, which includes the Sun, all planets, Pluto, the Moon, and 343 main-belt asteroids, and is consistent with JPL's DE430 model¹⁷; see Supplementary Note 1 for details and Supplementary Figure 1 for some comparisons.

For the treatment of the NEA, we consider Apophis as a massless test-particle subject to the Newtonian gravitational attraction from the Sun, the eight planets, the Moon, Pluto and the 16 most massive main-belt asteroids (see Supplementary Table 1), including post-Newtonian corrections (except for the asteroids) and Earth's J_2 zonal harmonic; see Supplementary Note 2. The choice of 16 asteroids is to have a fair comparison with other models^{6,13,17}, though not all these models use the most massive asteroids. More importantly, the model also comprises the Yarkovsky effect on Apophis as an acceleration along the transverse direction of motion, $\mathbf{a}_t = A_2 (r_0/r_{\text{Sun}})^2 \hat{\mathbf{t}}$, where $r_0 = 1$ au, r_{Sun} is the heliocentric distance expressed in au, and $\hat{\mathbf{t}}$ is the heliocentric unit transverse vector, which depends upon the velocity. Our goal is to determine the unknown proportionality constant A_2 which fits the optical and radar astrometry, based on precise numerical integrations of the equations of motion¹⁸. This coefficient allows one to estimate the associated semi-major axis drift⁶, $\langle \dot{a} \rangle = 2A_2(1 - e^2)r_0^2/(np^2)$, where n is the mean motion, e is the eccentricity, $p = a(1 - e^2)$ is the semi-latus rectum and a is the semi-major axis of Apophis. All parameters (planetary masses, zonal harmonics, etc.) used in our integrations (cf. Methods sections) are taken from the JPL DE430 ephemeris documentation¹⁷. We select initial conditions for our integrations from JPL's #197 solution for Apophis¹², at the epoch December 17, 2020 00:00:00.0 (TDB).

The results discussed below include the whole radar astrometry measurement data sets spanning from 2005 through 2013^{5,12}, as

well as three time-delays and a Doppler shift from observations of the recent Apophis flyby, obtained at Goldstone in early March 2021. In addition, we included 7,902 right-ascension/declination astrometry observation pairs, which span from March 15th, 2004 through May 12th, 2021; these data are available through the Minor Planet Center observational database¹⁹. Apart from a set of observations performed on January 28, 2021, which we excluded due to clear systematic bias, we have included essentially all the publicly-available ground-based optical astrometry for Apophis. Systematic errors due to timing, observational technique, reference star catalogs, etc., induce correlations in the orbital solution^{20,21}, which in turn bias the results²². To account for these biases, our optical astrometry error model considers appropriate star catalog debiasing techniques²³, and a suitable weighting scheme²⁴ which accounts for sources of systematic errors other than star catalog biases. See Supplementary Note 4 for further details.

We have produced two orbital fits to the astrometry data described above: a 6 degrees-of-freedom (DOF) gravity-only solution which uses a fixed value zero for the Yarkovsky parameter A_2 , the OR6 solution, and a 7-DOF non-gravitational solution, which fully takes into account the Yarkovsky effect, the OR7 solution. The results are presented in Figs. 1 and 2; see also Supplementary Note 5. Optical astrometry residuals for the gravity-only solution display a clear bimodal (two mode) distribution, which is not present for the corresponding residuals of the non-gravitational solution. As illustrated by the frequency histograms of right-ascension and declination residuals, upper and right panels of Fig. 1, the purple distributions have two bumps. These follow from the two clusters of (purple) points illustrated in the main panel. Therefore, since we expect the residuals to follow a Gaussian distribution, we interpret these bimodal distributions as an indication that the gravity-only solution is not compatible with the observational dataset. Moreover, as illustrated in Fig. 2 the radar astrometry residuals for the gravity-only solution (purple circles) display statistically significant offsets, while the corresponding radar astrometry residuals offsets from the non-gravitational solution are

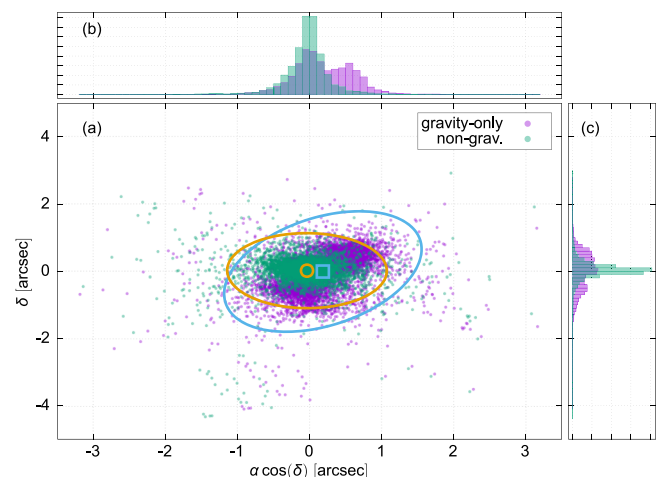


Fig. 1 Optical astrometry observed-minus-computed residuals. **a** The horizontal axis corresponds to right-ascension residuals and the vertical to declination residuals. Purple circles correspond to the residuals obtained from the gravity-only solution ($A_2 = 0$), and the average residual is illustrated as a blue square. Green circles correspond to the non-gravitational solution residuals; their average is marked with an orange circle. The ellipses centered at each average residual value represent the $3\text{-}\sigma$ level confidence. **b** Frequency histogram of right-ascension residuals. **c** Frequency histogram of declination residuals. Notice that the purple histograms display bimodal (two mode) distributions.

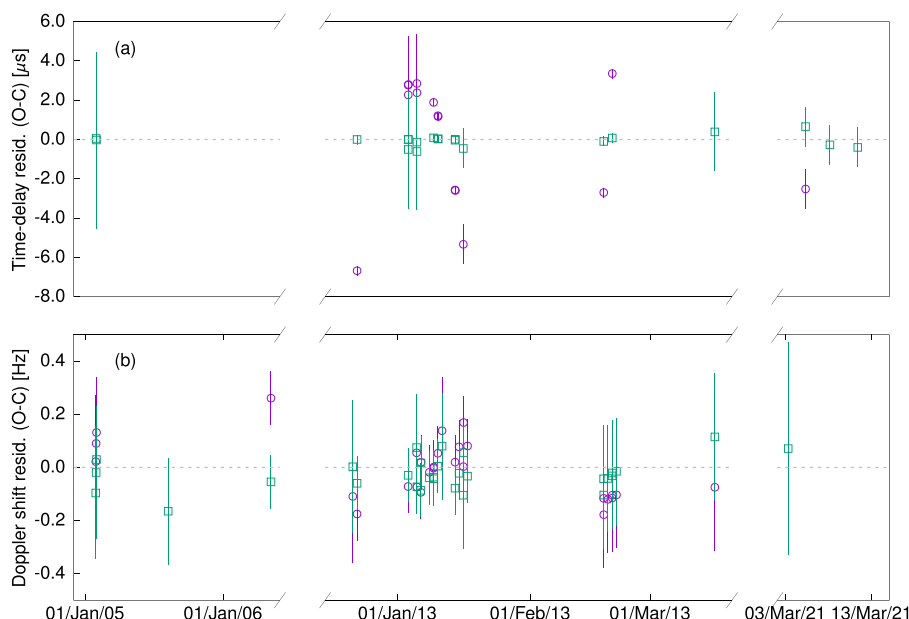


Fig. 2 Goldstone and Arecibo radar astrometry residuals in time. **a** Time-delay and **b** Doppler-shift residuals. Purple circles correspond to the gravity-only solution, while green squares correspond to the non-gravitational solution. The horizontal axis corresponds to the observation date; notice that it has a different scale in each segment of the plot. Error bars represent observational uncertainties. The residuals corresponding to the non-gravitational solution, together with their uncertainties, are compatible with zero; this is not the case for all gravity-only residuals.

Table 1 Fit quality statistics for the OR6 gravity-only and OR7 non-gravitational orbital solutions.

Post-fit measure	OR6	OR7
Normalized RMS (optical)	0.489	0.306
Normalized RMS (radar)	15.116	0.387
Normalized RMS (optical and radar)	0.979	0.306
Weighted mean R.A.	0.096"	0.006"
Weighted mean Dec.	0.082"	0.004"
Weighted mean time-delay	-0.07 μ s	-0.0003 μ s
Weighted mean Doppler shift	0.026 Hz	-0.0309 Hz
χ^2 ($\times 10^{-3}$)	15.205	1.482

smaller and all consistent with zero. These results can be cast in quantitative terms using the post-fit normalized RMS, mean weighted residuals and χ^2 , provided in Table 1. Clearly, the non-gravitational solution OR7 provides a more consistent fit to the radar and optical astrometry data.

Our estimate of the Yarkovsky transverse parameter obtained from the non-gravitational solution is $A_2 = (-2.899 \pm 0.025) \times 10^{-14} \text{ au d}^{-2}$, which yields a Yarkovsky-induced semi-major axis drift of $\langle \dot{a} \rangle = (-199.0 \pm 1.5) \text{ m yr}^{-1}$; the specific initial conditions and orbital elements for the solutions obtained are provided in Supplementary Tables 2 and 3. Therefore, our results show clearly a non-gravitational acceleration acting upon Apophis, due to the Yarkovsky effect. The value obtained for the Yarkovsky transverse parameter practically coincides with the current value reported at the JPL Small-Body Database for Apophis¹, namely $A_2^{\text{JPL}} = (-2.901 \pm 0.019) \times 10^{-14} \text{ au d}^{-2}$. In addition, it is consistent with preliminary results which incorporate high-quality optical astrometry¹⁵. Notice that the value reported¹⁵ for $\langle \dot{a} \rangle$ does not quite match the value we obtain; it is difficult to comment on this due to the lack of details on this estimate.

Based on these results, we turn now to the assessment of the collision probability for the close approach that will take place in April 13th, 2029. In Fig. 3 we plot the probability density of Öpik’s ζ coordinate on the 2029 b -plane, which is related to the arrival times

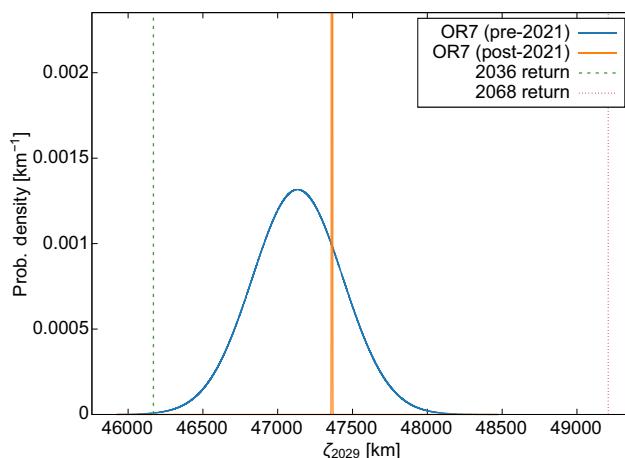


Fig. 3 Probability distribution of ζ_{2029} . Probability distribution on the 2029 b -plane due to the uncertainty in the non-gravitational orbital solution, which includes the Yarkovsky effect, with (orange line) and without (blue line) including the 2021 optical and radar astrometry. The vertical dashed and dotted lines represent, respectively, the ζ coordinate value on the 2029 b -plane corresponding to a resonant return in 2036 and 2068.

of the NEA²⁵. The figure displays the non-gravitational solution computed with the data available before the 2021 fly-by (blue curve, which yields²⁶ $A_2 = (-4.97 \pm 2.75) \times 10^{-14} \text{ au d}^{-2}$), and the corresponding solution which also includes the data gathered during the 2021 fly-by (orange curve). The histogram obtained with the 2021 data corresponds to a very narrow distribution around $\zeta_{2029} = 47,363 \text{ km}$. This rules out a collision event on April 13, 2029, and allows us to estimate a closest-approach distance of $(38,011.8 \pm 1.6) \text{ km}$ ($1\text{-}\sigma$ formal uncertainty). In Fig. 3 we have also included the estimated ζ values which correspond to possible future impacts during the close approaches in 2036 and 2068; these values were obtained from the resonant circles on the 2029 b -plane using jet transport techniques; details are included in Supplementary Note 6. The values corresponding to these events are located, respectively, at

–756 σ and 1163 σ , with respect to the nominal prediction and therefore their probability of occurrence is negligible. Yet, these results should be revisited in the future to incorporate new observations which will refine the quality of the fit that defines the nominal orbit and hence the collision assessment.

We also considered the dependency of A_2 in terms of the number of main-belt asteroids used in the dynamical model. The results presented use perturbations from the 16 most massive asteroids in the main belt. If we instead consider the gravitational perturbations on Apophis from the 32 most massive main-belt asteroids, the change in A_2 corresponds to 0.002σ with respect to the orbital fit obtained with 16 asteroids; σ denotes the uncertainty in A_2 . In terms of $\langle \dot{a} \rangle$, the difference is 0.003 m yr^{-1} . Öpik's ζ coordinate on the 2029 b -plane, ζ_{2029} , is shifted by 2 m, while the ζ values corresponding to resonant returns in 2036 and 2068 change by -0.6 km and 2.5 km , respectively.

We also considered an 8-DOF orbital fit which, in addition to the initial conditions and the Yarkovsky effect, estimates the non-gravitational acceleration due to the direct solar radiation pressure¹³ in the force model of Apophis. We model this acceleration as $\mathbf{a}_r = A_1 (r_0/r_{\text{Sun}})^2 \hat{\mathbf{r}}$, where $\hat{\mathbf{r}}$ is the radial unit vector, which is characterized by the radial non-gravitational parameter A_1 . The uncertainty associated with the value we obtain is large and comparable to the magnitude of A_1 , and therefore it only represents a marginal detection. The lack of a proper constrain of the uncertainty of A_1 can be attributed to the dataset itself, which may require more high-quality observations¹⁵. We have not pursued this any further. We note that recent computations by JPL¹ report the value $A_1^{\text{JPL}} = (5 \pm 4.903) \times 10^{-13} \text{ au d}^{-2}$.

Summarizing, using automatic differentiation techniques together with optical and radar astrometry we have obtained an orbital solution with a non-zero Yarkovsky transverse parameter for Apophis, including its uncertainty. High-order automatic differentiation is exploited to obtain the actual orbits, the fit to data of the nominal A_2 value and initial conditions, the corresponding semimajor axis drift, and for the uncertainty calculations. The solution obtained provides qualitatively and quantitatively better O-C residuals than the one which includes only a gravitational interaction, i.e., which assumes a zero value for the Yarkovsky parameter. The acceleration associated with the Yarkovsky effect induces a semi-major axis drift of $\langle \dot{a} \rangle = (-199.0 \pm 1.5) \text{ m yr}^{-1}$. Moreover, this non-gravitational solution allows us to predict a closest-approach distance of $(38,011.8 \pm 1.6) \text{ km}$ ($1\text{-}\sigma$ formal uncertainty) on April 13, 2029. We have also analyzed the orbital uncertainty on the 2029 b -plane to conclude that this close approach will not lead to impacts on neither 2036 nor 2068, though a more refined analysis is required to discard the possibility of impacts in the next 200 years. The consistency of these results with other estimations using also data from 2021^{1,15} serves as an independent validation, which is important for potentially hazardous asteroids.

Methods

The integration of the differential equations uses a variable step-size 25-order Taylor integration method for the planetary ephemeris and for Apophis orbit, with a small absolute tolerance (10^{-20}). An additional differential equation is added for the Yarkovsky parameter, $\dot{A}_2 = 0$, which assumes the constancy of Yarkovsky parameter as a first approximation, and allows one to consider small variations around an a priori nominal value of A_2 , which initially is set to zero. The numerical integration of Apophis¹⁸, besides considering the nominal initial conditions and the nominal A_2 , also integrates small deviations from these nominal values. These deviations are included as truncated polynomials in the small deviations, up to order 5, and are transported along the integration in time; see Supplementary Note 3, for details. At each step of the numerical integration we compute polynomials in time for the positions and velocities of all the Solar System objects considered. For Apophis, the coefficients of those polynomials are polynomials in the small deviations from the nominal values of the initial conditions and Yarkovsky parameter. These series expansions, combined with radar and optical

astrometry data, allow us to obtain the optimal deviations from the nominal values by minimizing the observed-minus-computed (O-C) residuals. The optimal deviations in the unknown parameters are obtained through a Newton iterative method, which exploits the derivatives of the polynomials that the integration produce. We further exploit automatic differentiation when constructing the covariance matrix used to compute the uncertainty of A_2 and the initial conditions. The covariance matrix is the inverse of the Hessian, which is obtained directly from the explicit time series produced by our integrator. In this sense, we include non-linear terms which are ignored when the covariance matrix is constructed from the transition-state matrix. The numerical stability of our results was addressed by contrasting them against JPL's #197 solution¹², a gravity-only solution.

Data availability

The astrometry used to obtain the results of this paper can be found at <https://github.com/PerezHz/NEOs.jl>, under the data directory. Optical astrometry was retrieved from <https://minorplanetcenter.net>¹⁹ and radar astrometry from <https://ssd.jpl.nasa.gov/sb/radar.html>.

Code availability

All code used to obtain the results presented in this paper is in the public domain and was developed by the authors. The (Julia) package `PlanetaryEphemeris.jl`¹⁶ is available in <https://github.com/PerezHz/PlanetaryEphemeris.jl> and `NEOs.jl`¹⁸ in <https://github.com/PerezHz/NEOs.jl>.

Received: 16 August 2021; Accepted: 16 December 2021;

Published online: 11 January 2022

References

- JPL Small-Body Database (data for Apophis). https://ssd.jpl.nasa.gov/tools/sbdb_lookup.html#/?sstr=Apophis. Accessed: 03-10-2021.
- Chesley, S. R. Potential impact detection for Near-Earth asteroids: the case of 99942 Apophis (2004 MN 4). In *Asteroids, Comets, Meteors, Proceedings of IAU Symposium* (eds Lazzaro, D., Ferraz-Mello, S. & Fernández, J. A.) Vol. 229, 215–228 (2006).
- Scheeres, D. et al. Abrupt alteration of Asteroid 2004 MN4's spin state during its 2029 Earth flyby. *Icarus* **178**, 281–283 (2005).
- Farnocchia, D. et al. Near Earth asteroids with measurable Yarkovsky effect. *Icarus* **224**, 1–13 (2013).
- Giorgini, J., Benner, L., Ostro, S., Nolan, M. & Busch, M. Predicting the Earth encounters of (99942) Apophis. *Icarus* **193**, 1–19 (2008).
- Farnocchia, D. et al. Yarkovsky-driven impact risk analysis for asteroid (99942) Apophis. *Icarus* **224**, 192–200 (2013).
- Vokrouhlický, D. et al. The Yarkovsky effect for 99942 Apophis. *Icarus* **252**, 277–283 (2015).
- Vokrouhlický, D., Milani, A. & Chesley, S. Yarkovsky effect on small near-Earth asteroids: Mathematical formulation and examples. *Icarus* **148**, 118–138 (2000).
- Giorgini, J. et al. Asteroid 1950 DA's encounter with Earth in 2880: physical limits of collision probability prediction. *Science* **296**, 132–136 (2002).
- Botke Jr, W. F., Vokrouhlický, D., Rubincam, D. P. & Nesvorný, D. The Yarkovsky and YORP effects: Implications for asteroid dynamics. *Annu. Rev. Earth Planet. Sci.* **34**, 157–191 (2006).
- Chesley, S. R. et al. Orbit and bulk density of the OSIRIS-REx target asteroid (101955) Bennu. *Icarus* **235**, 5–22 (2014).
- Brozović, M. et al. Goldstone and Arecibo radar observations of (99942) Apophis in 2012–2013. *Icarus* **300**, 115–128 (2018).
- Del Vigna, A. et al. Detecting the Yarkovsky effect among near-Earth asteroids from astrometric data. *Astronomy & Astrophysics* **617**, A61 (2018).
- Greenberg, A. H., Margot, J.-L., Verma, A. K., Taylor, P. A. & Hodge, S. E. Yarkovsky drift detections for 247 near-Earth asteroids. *The Astronomical Journal* **159**, 92 (2020).
- Tholen, D. & Farnocchia, D. Detection of yarkovsky acceleration of (99942) apophis. In *AAS/Division for Planetary Sciences Meeting Abstracts*. Vol. 52, 214–06 (2020).
- Pérez-Hernández, J. A. & Benet, L. PlanetaryEphemeris.jl: A planetary and lunar ephemerides integrator based on JPL DE430 dynamical model. <https://github.com/PerezHz/PlanetaryEphemeris.jl> (2021). <https://doi.org/10.5281/zenodo.5152452>.
- Folkner, W., Williams, J., Boggs, D., Park, R. & Kuchynka, P. The planetary and lunar ephemerides DE430 and DE431. *Interplanet. Netw. Prog. Rep* **196**, 1–81 (2014).
- Pérez-Hernández, J. A. & Benet, L. NEOs.jl: Jet Transport-based Near-Earth Object orbital propagator and fitter in Julia. <https://github.com/PerezHz/NEOs.jl>; <https://doi.org/10.5281/zenodo.5152449> (2021).
- Minor Planet Center orbits and observations database. <https://minorplanetcenter.net>. Accessed: 08-03-2021.

20. Carpino, M., Milani, A. & Chesley, S. R. Error statistics of asteroid optical astrometric observations. *Icarus* **166**, 248–270 (2003).
21. Chesley, S. R., Baer, J. & Monet, D. G. Treatment of star catalog biases in asteroid astrometric observations. *Icarus* **210**, 158–181 (2010).
22. Królikowska, M., Sitarski, G. & Sołtan, A. M. How selection and weighting of astrometric observations influence the impact probability. The case of asteroid (99942) Apophis. *Mon. Not. R. Astron. Soc.* **399**, 1964–1976 (2009).
23. Eggl, S., Farnocchia, D., Chamberlin, A. B. & Chesley, S. R. Star catalog position and proper motion corrections in asteroid astrometry II: The Gaia era. *Icarus* **339**, 113596 (2020).
24. Vereš, P., Farnocchia, D., Chesley, S. R. & Chamberlin, A. B. Statistical analysis of astrometric errors for the most productive asteroid surveys. *Icarus* **296**, 139–149 (2017).
25. Valsecchi, G. B., Milani, A., Gronchi, G. F. & Chesley, S. R. Resonant returns to close approaches: analytical theory. *Astronomy & Astrophysics* **408**, 1179–1196 (2003).
26. Pérez-Hernández, J. A. Dynamics of Near-Earth Objects: the Yarkovsky Effect for Asteroid Apophis and the Lyapunov Spectrum of Halley's Comet. Ph.D thesis (Universidad Nacional Autónoma de México (UNAM), 2021).

Acknowledgements

The authors are thankful to Davide Farnocchia (JPL) for correspondence and valuable insights, W. Folkner (JPL) for his assistance with the fine details related to the JPL DE430/431 ephemeris and Lázaro Alonso for his help in producing the figures. We are also thankful to the referees, whose comments and suggestions greatly improved the manuscript. This research has made use of data and/or services provided by the International Astronomical Union's Minor Planet Center. We acknowledge financial support from the PAPIIT-UNAM project IG-100819, and computer time provided through the project LANCAD-UNAM-DGTIC-284.

Author contributions

J.A.P.H. wrote most of the code, performed the numerical simulations and their subsequent reduction. L.B. designed the original project. Both authors contributed to the analysis of the results and writing the paper.

Competing interests

The authors declare no competing interests.

Additional information

Supplementary information The online version contains supplementary material available at <https://doi.org/10.1038/s43247-021-00337-x>.

Correspondence and requests for materials should be addressed to Jorge A. Pérez-Hernández or Luis Benet.

Peer review information *Communications Earth & Environment* thanks Giovanni Valsecchi, Alessio Del Vigna and the other, anonymous, reviewer for their contribution to the peer review of this work. Primary Handling Editors: Joe Aslin, Heike Langenberg. Peer reviewer reports are available.

Reprints and permission information is available at <http://www.nature.com/reprints>

Publisher's note Springer Nature remains neutral with regard to jurisdictional claims in published maps and institutional affiliations.



Open Access This article is licensed under a Creative Commons Attribution 4.0 International License, which permits use, sharing, adaptation, distribution and reproduction in any medium or format, as long as you give appropriate credit to the original author(s) and the source, provide a link to the Creative Commons license, and indicate if changes were made. The images or other third party material in this article are included in the article's Creative Commons license, unless indicated otherwise in a credit line to the material. If material is not included in the article's Creative Commons license and your intended use is not permitted by statutory regulation or exceeds the permitted use, you will need to obtain permission directly from the copyright holder. To view a copy of this license, visit <http://creativecommons.org/licenses/by/4.0/>.

© The Author(s) 2022